ISSN 1068-3755, Surface Engineering and Applied Electrochemistry, 2016, Vol. 52, No. 5, pp. 449–455. © Allerton Press, Inc., 2016.

Adsorption of Atmospheric Carbonate and Evolution of Acidity during Grinding of Abnormal Montmorillonite[1]

I. Bekri-Abbes* and E. Srasra

Laboratoire de Physico-chimie des Matériaux Minéraux et leurs Applications, Centre National de Recherches en Sciences des Matériaux, Borj Cedria, Tunis, Tunisia

**e-mail: bekrimene@gmail.com*

Received March 30, 2015

Abstract– Montmorillonite (MMt) from Tunisia has been subjected to fine grinding and studied using FTIR spectroscopy, X-ray diffractograms, BET surface area, Brönsted and Lewis acidity analyse, and FTIR spectroscopy. As a result, significant changes in structural vibrations when MMt was mechanochemically treated were revealed. These changes include: a shift and a gradual decrease of structural OH, Si–O, and M–OH groups (M: octahedral cations; Al, Mg and Fe), which means that an imperfection was formed in the crystal mineral via a mechanochemical treatment. The grinding is associated with amelioration of the oxidative power of clay, which is manifested by the sharpening of the infrared absorption shoulder near 880 cm^{-1}. The thermo-FTIR adsorption of N-butylamine showed that acidity did not improve upon grinding. On the contrary, the mechanochemical treatment led to the creation of the basic sites which promote the adsorption of atmospheric dioxide carbon.

Keywords: grinding, FTIR spectroscopy, Brönsted acidity, Lewis acidity, Brunauer–Emmett–Teller method

DOI: 10.3103/S1068375516050045

INTRODUCTION

Smectite group minerals are 2 : 1 type layered clay minerals. Montmorillonite (MMt), the object of the study here, is a dioctahedral smectite in which only two of the three octahedral sites of the half unit cell are occupied, which leads to vacant sites in *cis* positions (a normal MMt) or vacant sites in *trans* position (an abnormal MMt) (Fig. 1) [1]. Depending on the configuration, physical and chemical properties of MMts differ. For example, most MMts (*cis* vacant or normal MMt) are more stable thermally than an abnormal MMt [2]. MMt has been widely used for the preparation of inorganic–organic nanocomposites due to its high cation exchange capacity, swelling ability, and wide surface area. During the past three decades, the preparation of nanocomposites by a mechanochemical reaction [3–5] was in the focus of attention of researchers. A mechanochemical reaction is realized via grinding clay minerals and organic substances using ball milling or a grinder mortar. It was shown that the structure of the polymer-clay nanocomposites prepared by the mechanochemical reaction differs from that of a nanocomposite synthetized by a conventional solution method.

This effect has been attributed to the alteration of the clay structure under grinding [4]. The effect of grinding on the structure of a normal MMt has been widely studied [6–9]. In most cases, grinding causes delamination at the initial stages followed by the destruction of the structure and subsequent amorphization, associated with the re-aggregation of the mineral grains. However, to the best of our knowledge, the mechanochemical effect on anabnormal MMt has never been studied. Thus, the present study deals with the characterization of the effect of grinding on acidity and physico-chemical properties of an abnormal MMt from Tunisia.

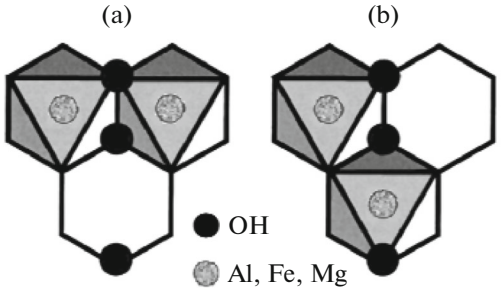

Fig. 1. Schematic presentation of an octahedral sheet and distribution of octahedral cations with *trans*- (a) and *cis*-vacant sites (b).

[1] The article is published in the original.

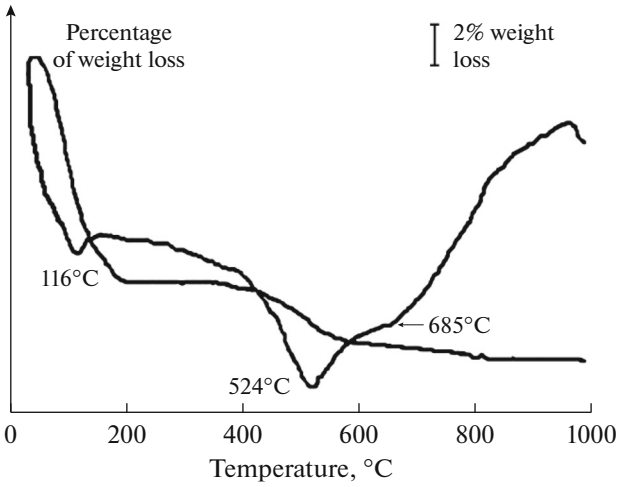

Fig. 2. DTA and TGA curves of abnormal MMt.

EXPERIMENTAL

The MMt used in the present study is natural clay from Zaghouan in Tunisia. The chemical composition of the sample in mass (%) was: MgO, 3.95; CaO, 0.28; SiO_2, 50.08; Fe_2O_3, 6; K_2O, 0.84; Al_2O_3, 17.4. and loss on ignition was 21.4. A sodium MMt was prepared via purification of crude clay and its further exchange with NaCl solution. Fine grinding was performed in a Retsch mortar grinder while varying time and fixing the pressure and mass of the clay to 0.5 g. According to the periods of treatment, the samples were identified as Mn, where the subscripts indicate the treatment time in minutes.

The X-ray diffractograms were obtained on a Panalytical diffractometer using Cu Kα radiation. The infrared (IR) spectra were obtained with a Nicolet spectrophotometer, model 560, with a scanning range between 400 and 4000 cm^{-1}. The samples were prepared as tablets diluted in KBr, keeping constant the sample/KBr ratio and the total weight of the sample. The thermal analysis was performed in an air atmosphere with a Netzsch STA-409 EP instrument at the heating rate of 10°C/min. The specific surface area was determined by applying the Brunauer-Emmett-Teller (BET) method using an automatic adsorption instrument (Autosorb I). Prior to the analysis, the samples were outgassed at 150°C for 2h.

The surface acidity (Brönsted and Lewis acid centres) was determined by the Fourier-transform infrared spectroscopy (FTIR spectroscopy) on the basis of adsorption of N-butylamine: 1 mL of N-butylamine solution was added to 0.1 g of clay. The mixture was shaken at room temperature. After drying, each sample was calcined at different temperatures, ranging from 200 to 800°C, and characterized by the FTIR spectroscopy [10].

RESULTS AND DISCUSSIONS

Characterization of Abnormal MMt

The use of the thermal analysis together with the IR spectroscopy permits identification of the *cis* and *trans* vacant MMts [11]. The thermogravimetric analysis (TGA) of the clay used in this study shows the appearance of two weight losses: the first one localized at 116°C is attributed to the adsorbed water and moisture. The specific weight loss in this reaction is about 10.3%. The difference between the normal and abnormal MMts can be observed in the 400–800°C range where deshydroxylation occurs. In fact, MMts are characterized by a wide range of deshydroxylation temperatures from 500°C to 700°C. Most MMts (*cis* vacant or normal MMt) have one endothermic peak near 720°C whereas only a few MMts (*trans* vacant or abnormal MMt) show two peaks near 500 and 680°C [11]. Figure 2 demonstrated that the deshydroxylation of thissample shows double peaks: one at 524°C (weight loss of 2.4%) and the second at 678°C (about 0.6% weight loss). The data obtained by the thermal analysis suggests that this MMt has *trans* vacant octahedral sites. More confirmation could beobtained by the IR spectroscopy. The MMt spectrum (Fig. 3) presents absorption bands at 1040 cm^{-1} (Si–O stretching vibrations), 526 cm^{-1} (Si–O–Al), 472 cm^{-1} (Si–O–Si bending vibrations); 916 cm^{-1} and 836 cm^{-1} are due to Al(III)–OH and Mg–OH bending vibrations, respectively. The absorption bands at 3426 cm^{-1} and 1634 cm^{-1} correspond, respectively, to the stretching and bending vibration absorption of the O-H bond of water. Small quantities of quartz are detected by the doublet at 778 and 800 cm^{-1}. The difference between normal and abnormal MMts can be established in the range of vibrations of structural hydroxyls and lattice vibrations [11]. In fact, in the range of OH stretching vibrations, a normal MMt shows a medium absorption band in the interval of 3625–3636 cm^{-1}, which is attributed to the hydroxyl coordinated to (Al, Al) pairs; however, the interval of absorption of this band for an abnormal MMt is between 3610 and 3621 cm^{-1} [11]. As shown in Fig. 3 this band is seen at 3622 cm^{-1}. In addition, the spectrum shows the appearance of a shoulder at 426 cm^{-1}. As reported in literature [11], all abnormal samples showed an absorption band resembling a shoulder at about 420–425 cm^{-1}, which is not observed in the spectra of normal MMts. That band is associated with a high proportion of Fe^{3+} in octahedral sites.

Adsorption of Atmospheric Carbonate and Evolution of Acidity during Grinding of MMt

The X-ray diffractogramms of the untreated and treated samples are given in Fig. 4. A significant broadening and decrease of 00l peak were observed with a longer grinding time. This observation supports

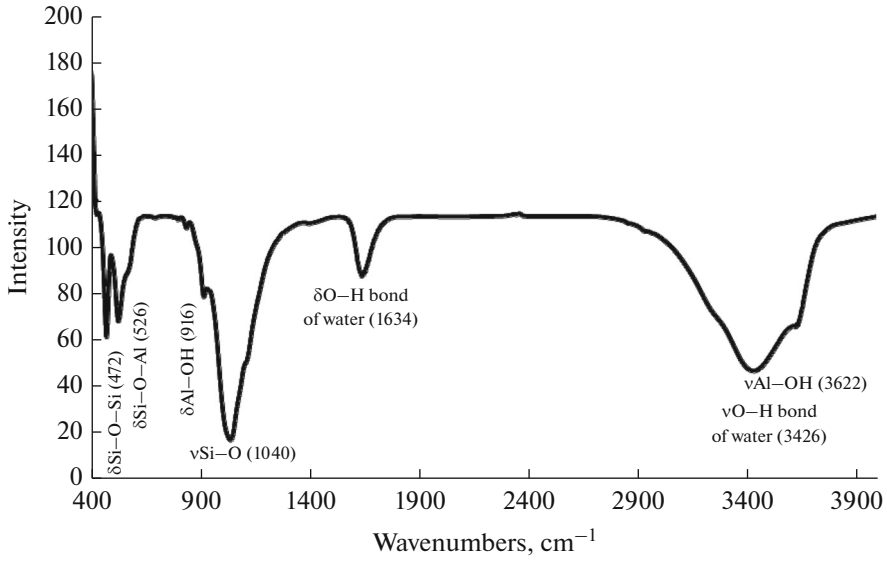

Fig. 3. FTIR spectrum of the abnormal MMt.

earlier works [7–9]. On the contrary, the *d* 060 peak only decreased after a prolonged grinding of 60 mn. Therefore, the intensity of the *d* 001 diffraction diminishes more rapidly than that of the *d* 060 diffraction as function of the grinding time. It seems that tangential forces predominate over perpendicular ones and the gliding of particles of 2 : 1 layers in the *ab* plane is more probably destructed than their structural decomposition in the *ac* or the *bc* plane as explained in Fig. 5. As shown in Table, the specific surface area of the ground samples is enlarged with the grinding time from 78.8 m^2/g for an untreated clay to 127.2 m^2/g in that ground for 30 minutes, and then decreased to 66.8 m^2/g in the sample ground for 75 minutes. The reduction of the surface area is directly influenced by the formation of aggregates with small particle sizes at short grin-ding times. The reduced specific surface area obtained at the longest grinding time must be the result of the formation of stable large aggregates. Some authors have found the specific surface area to enlarge at shorter grinding times and to reduce at longer grinding times [12, 13]. However, the reported in literature grinding time at which the trend in the variation of the specific surface changes varies from author to author, probably depending on the working conditions, the type of mill and amount of samples used in each operation. A rapid reduction of the specific surface area was reported when the grinding time increased for imogolite; at the same time, those authors wrote that

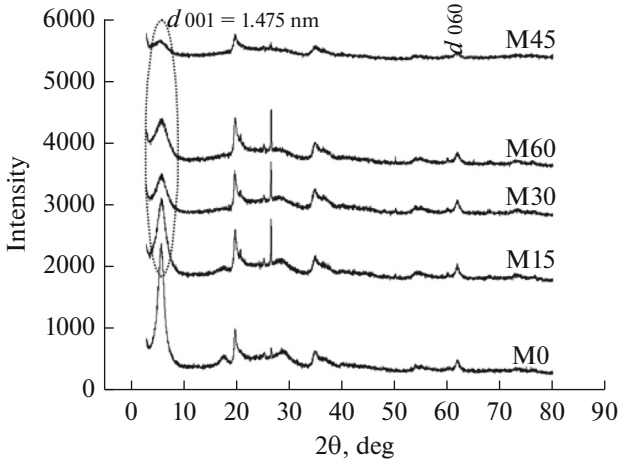

Fig. 4. X-ray diffractogramms of untreated and ground MMt.

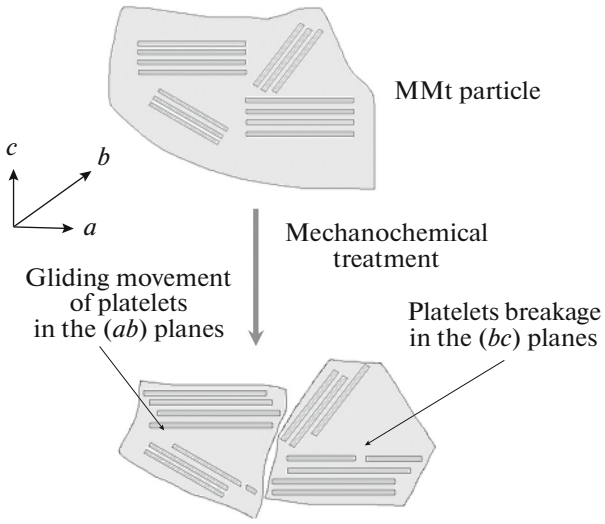

Fig. 5. Schematic representation of the reduction of particle size of clay, gliding movements and breakage of the MMt particles.

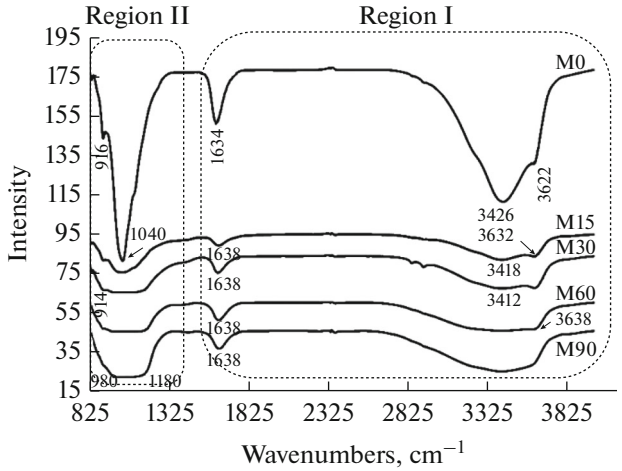

Fig. 6. FTIR spectra of untreated and ground MMt in regions I and II.

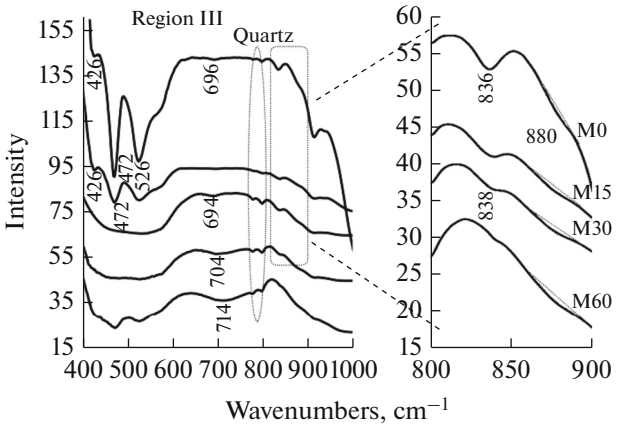

Fig. 7. FTIR spectra of untreated and ground MMt in region III.

the particle morphology changed from fibres to coarse aggregates [12]. The reduction of the measured surface area is caused by the collapse of the micropores of imogolite. During the first minute of grinding, there is a downsizing of the particles, which contributes to theenlargement of the specific surface area. With a prolonged grinding time, the aggregation of particles results in a shrinkage of the specific surface area. The process of agglomeration occurs naturally in powders and is caused essentially by adhesion forces that always act between the fine particles produced by grinding [14].

Structural changes due to the grinding of clay were monitored by changes in the following regions: Region I: 3400 to 3650 cm^{-1} and 1630–1640 cm^{-1}, associated with the O-H stretching vibrations of structural hydroxyl (Al–OH) and adsorbed water; Region II: 900–1200 cm^{-1} associated with the Si–O vibrations and Al–OH bending vibration; and Region III: 400–900 cm^{-1} associated with the M–O–H vibrations of octahedral cations (M = Fe, Al, or Mg) and 1300–1400 cm^{-1}.

The Al-OH stretching band in untreated MMts is found at 3622 cm^{-1} (Fig. 6), which is characteristic of Al–OH vibration; it shifts to a grater wavelength of about 3632, 3636 and 3638 cm^{-1} for M15, M30 and M60, respectively, and it disappears for M90. These features suggest that deshydroxylation may occur as a consequence of grinding. A broad band centered at about 3400 cm^{-1} appears. This band can be assigned to H_2O in the smectite structure. At least, two scenarios can be considered to explain the formation of this broad band, namely; (1) the hydration energy of the ground MMt is greater than that of an untreated MMt and structural OH groups are converted to structural H_2O groups during grinding. The H_2O molecules responsible for the large band at 3400 cm^{-1} in the ground samples could, therefore, be adsorbed to the basal surfaces of the smectite. (2) Another explanation for this strongly bound H_2O is caused by the connection of the bound water to the defects in the octahedral sheet rather than beingentirely at the basal surface. One more observation is related to the shift of the bending vibration of H_2O from 1634 to 1638 cm^{-1} for an untreated MMt.

Changes are also observed in the Si–O stretching region (1040 cm^{-1} for the untreated clay) (Fig. 6) including broadening and reduction of the intensity. Such changes indicate that grinding affects the structural properties of the tetrahedral sheet, which, in turn, results in changes of the physical and chemical properties at the mineral surface, such as the coupling of H_2O molecules with the basal oxygen surfaces of tetrahedral sheets. The band at 916 cm^{-1} is due to the Al(III)–O–H bending vibration. This band shifts downwards by about 2 cm^{-1} with increasing the grinding time, then its intensity decreases and it disappeares for M90. The weakening and then disappearing of this band indicate that OH groups, coordinating central atoms (mainly Al) in the octahedral sheets, were released and some octahedral sheets were damaged.

The intensity of the bands at 526 cm^{-1} and 472 cm^{-1} attributed to Si–O–Al and Si–O bending vibrations, respectively, decreased and they disappeared partly with the grinding time (Fig. 7), indica-ting a breakdown of the Si–O–Al bonds, namely, the destruction of the linkages between the octahedral and the tetrahedral sheets. On the other hand, the degradation of the Si–O bending vibration indicates that grinding

Evolution of specific surface area duringgrinding

Samples	M0	M15	M30	M45	M60	M75
Specific surface area (m^2/g)	78.8	98.2	127.2	111.7	87.5	66.8

affects tetrahedral sheets in the same manner. These results are supported by the X-ray difractogramms, showing a suggested damage of the crystalline structure of the MMt. It can be seen that in the region between 800 and 900 cm^{-1}, where, as a rule, a shoulder appears at around 880 cm^{-1} and which results from the Fe-OH-Al bending vibration. As shown in Fig. 7 (the right-hand side), this band appears at 880 cm^{-1} and then it shifts to 778 cm^{-1} with grinding.

This band comprises the Fe^{2+}–OH–Al and Fe^{3+}–OH–Al deformations. The grinding is associated with a slight sharpening and broadening of that shoulder. In general, the more oxidized the sample, the sharper the absorption in this region [15]. This analysis proves that grinding increases the oxidizing power of MMt. This observation has been noted by Keller (1955) [15] who observed a change of color of Cheto MMt and assumed an oxidation and conversion of ferrous to fericions MMt. An effect of mechanochemical treatment is the downsizing of clay particles and exposure of more surface edges to atmospheric oxygen that oxidizes structural Fe^{2+} to Fe^{3+}. A new broad band near 690–720 cm^{-1} appears in the spectra of the MMt ground for 30, 60, and 90 min. This band is frequently observed in the spectra of three-dimensional aluminosilicates such as zeolites (Phillipsite at 709 cm^{-1}, Harmotome at 729 cm^{-1}, and Gismondite at 712 cm^{-1}) [17] and is attributed to the symmetric stretching vibrations of bridge bonds Si–O–Si. This confirms the considerable decomposition of the layers and the formation of a bridge between Si–O groups of the broken tetrahedral layers.

Another attribution of this band could be caused by adsorbing the atmospheric CO_2 by the broken surface sites. Our supposition is supported by the appearance of a double band localized at 1386 cm^{-1} and 1402–1418 cm^{-1} (Fig. 8). It is well known that the carbonate vibrations are observed in the range 1400–1500 cm^{-1} [18]. The C-O antisymmetric stretching of CO_3^{2-} anion was observed at 1368 cm^{-1} [19]. More specifically, the υ3 mode (asymmetric stretching) of the CO_3^{2-} anions appears around 1404 cm^{-1}. In our case, the υ3 carbonate band splits into two separate bands at 1400 and 1386 cm^{-1} (Fig. 7). The same observation has been noted by the carbonate anion intercalated in hydrotalcite and anionic clays and it has been attributed to a rearrangement of the carbonate groups coordinated to hydroxyl groups of the octahedral brucite-like layers [20, 21]. It is well known that prolonged grinding of silicate minerals such as diopside ($CaMgSi_2O_6$) and okermanite ($Ca_2MgSi_2O_7$) in the air is accompanied by the adsorption of carbon dioxide from the atmosphere [22]. Carbon dioxide is homogeneously adsorbed by the minerals without the formation of individual crystal carbonate phases. The real mechanism for the adsorption of carbon dioxide during grinding of the abnormal MMt is not understood yet. However, we asuume that the adsorption of CO_2 is likely to be caused by basic sites that may originate from O^{2-} (these groups result probably from the reduction of atmospheric oxygen) and from broken hydroxyl groups.

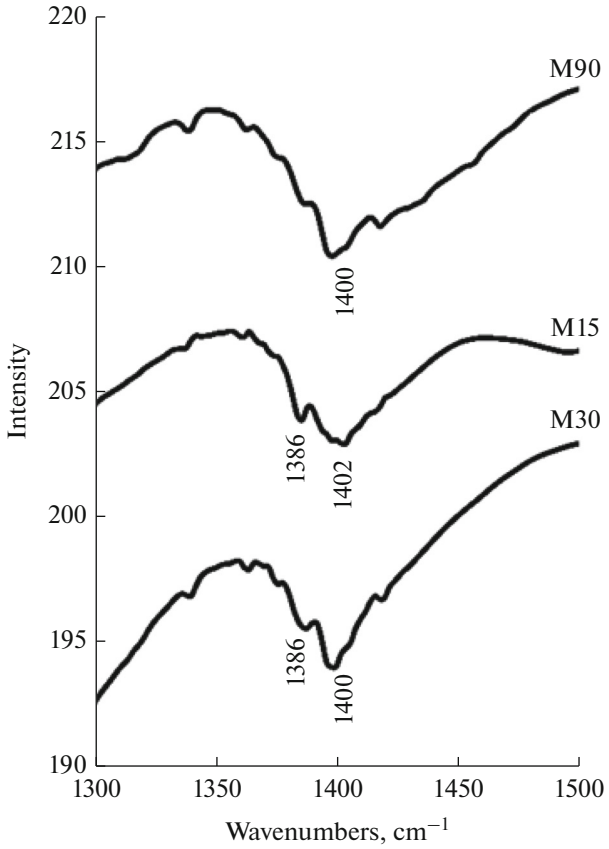

Fig. 8. FTIR spectra of untreated and ground clay in region III (1300–1500 cm^{-1}).

The surface acidity of clays can be measured from the extent to which adsorbed organic bases are protonated by the clay [23]. The evolution of acidity of clay minerals by FTIR thermo desoption of N-butylamine was studied by Mnasri et al. [10]. The technique involves the evolution of the FTIR spectrum of N-butylamine adsorbed by the sample as a function of temperature. In this way, it is possible to determine the nature of clay acid sites. Generally the following two types of acidity are typical for clays: Lewis acidity (around 1450 and 1590 cm^{-1}) and Brönsted acidity (in the range of 1545 cm^{-1}). The band which appears around 1490 cm^{-1} is mainlyattributed to both Lewis and Bronsted acidities. The IR spectra of N-butylamine adsorbed by the samples M0, M15, M30 and M60 are shown in Fig. 9. Untreated and ground clays present bands attributed to Lewis acidity. Bronsted acid sites were not found on any of the samples. Thus the grinding did not ameliorate the acidity of clay.

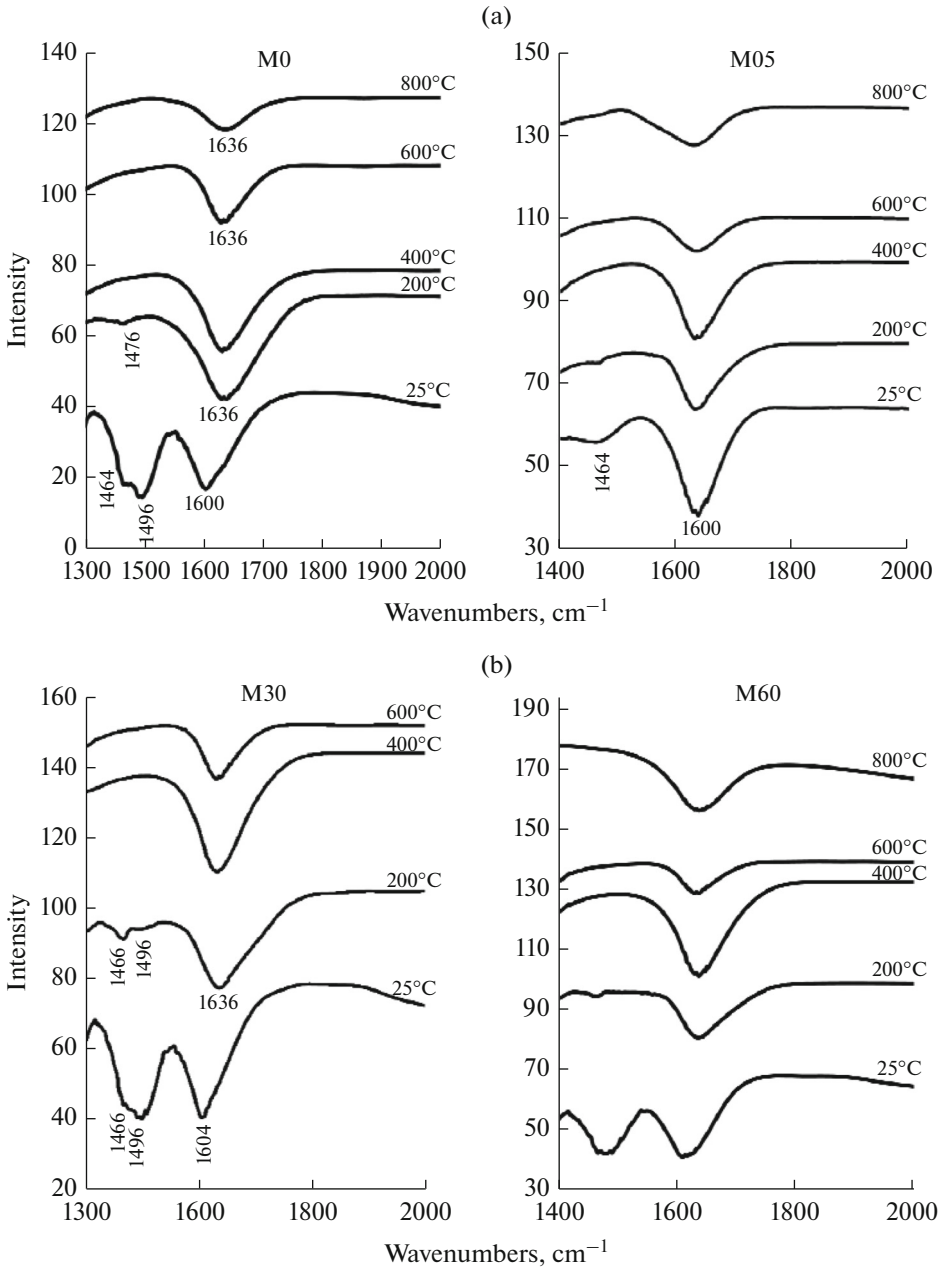

Fig. 9. FTIR spectra of IR spectra of N-butylamine adsorbed at untreated and ground clay at different temperatures in region 1400–2000 cm^{-1}.

Other researchers [24] studied acidic properties of sonicated clay particles using the basic dyes methylene blue and showed that sonication induces a delamination effect on the MMts and the acidic sites are eliminated during the treatment.

CONCLUSIONS

To sum up, an abnormal MMt was subjected to mechanochemical treatment using a mortar grinder. FTIR spectroscopy revealed increased significant changes in the spectrum of MMt upon grinding. Structural changes include a decrease in the structural OH content. Those sites from which structural OH groups are lost create a defect in the octahedral sheets. The grinding is accompanied by an increase of the oxidative power of the mineral, which is associated with a sharpening of the infrared absorption near 880 cm^{-1} due to Fe^{2+}–OH–Al and Fe^{3+}–OH–Al deformations. The oxidation of an octahedral iron reduces the charge on the MMt layers. The charge balance can be maintained either by deprotonation of structural hydroxyl groups or by a decrease in the amount of exchangeable

cations. From our studies, we deduce that the charge balance is maintained by deprotonation, resulting from the grinding accompanied by a decrease and disappearance of hydroxyl bending and stretching vibrations. The appearance of a band centered at 700 cm^{-1} and small double bands around 1400 cm^{-1} proved that the grinding of an abnormal MMt is accompanied by adsorption of atmospheric CO_2. Those molecules were adsorbed on the electron-donor sites derived from the broken OH groups at crystal edges from external OH groups bearing a negative charge or from O_2^- produced from the reduction of atmospheric oxygen. The evolution of FTIR spectra of N-butylamine adsorbed on the ground clay proved that acidity did not ameliorate with grinding.

ACKNOWLEDGMENTS

The authors gratefully acknowledge the financial support provided by the Higher Education and Scientific Research Sector of the Ministry of Higher Education, Scientific Research and Information and Communication Technologies of Tunisia.

REFERENCES

1. Drits, V.A., Besson, G., and Muller, F., *Clay Clay Miner.*, 1995, vol. 43, pp. 718–731.
2. Grim, R.E. and Kulbicki, G., *Am. Miner.*, 1961, vol. 46, pp. 1329–1369.
3. Bekri-Abbes, I. and Srasra, E., *Bull. Mater. Sci.*, 2006, vol. 29, pp. 251–259.
4. Bekri-Abbes, I. and Srasra, E., *J. Polym. Res.*, 2011, vol. 18, pp. 691–699.
5. Bekri-Abbes, I. and Srasra, E., *React. Funct. Polym.*, 2010, vol. 70, pp. 11–18.
6. Cicel, B. and Kranz, G., *Clay Miner.*, 1981, vol. 16, pp. 151–162.
7. Mingelgrin, U., Kliger, L., Gal, M., and Saltzman, S., *Clay Clay Miner.*, 1978, vol. 26, pp. 299–307.
8. Hrachova, J., Madejova, J., Billik, P., and Komadel, P., *J. Colloid Interf. Sci.*, 2007, vol. 316, pp. 589–595.
9. Ramadan, A.R., Esawi, A.M.K., and Gawad, A.A., *Appl. Clay Sci.*, 2010, vol. 47, pp. 196–202.
10. Mnasri, S. and Frini-Srasra, N., *Infrared Phys. Techn.*, 2013, vol. 58, pp. 15–20.
11. Craciun, C., *Thermochim. Acta*, 1987, vol. 117, pp. 25–36.
12. Henmi, T. and Yoshinaga, N., *Clay Miner.*, 1981, vol. 1, pp. 139–149.
13. Cornejo, J. and Hermosin, M.C., *Clay Miner.*, 1988, vol. 23, pp. 391–398.
14. Rumpf, H. and Schubert, H., Adhesion forces in agglomeration processes, in *Ceramic Processing before Firing*, Onoda, G. and Hench, L., Eds., New York: Wiley, 1978, pp. 357–376.
15. Rozenson, I. and Heller-Kallai, L., *Clay Clay Miner.*, 1978, vol. 26, pp. 8–92.
16. Keller, W.D., *Am. Miner.*, 1955, vol. 40, pp. 348–351.
17. Mozgawa, W., Krol, M., and Barczy, K., *Chemik*, 2011, vol. 7, pp. 671–674.
18. Freund, H.J. and Roberts, M.W., *Surf. Sci. Rep.*, 1996, vol. 25, pp. 225–273.
19. Chappell, B.W. and White, A.J.R., *Pac. Geol.*, 1974, vol. 8, pp. 173–174.
20. Melian-Cabrera, I. and Granados, M.L., *Phys. Chem. Chem. Phys.*, 2002, vol. 4, pp. 3122–3127.
21. Hibino, T., Yamashita, Y., Kosuge, K., and Tsunashim, A., *Clay Clay Miner.*, 1995, vol. 43, pp. 427–432.
22. Kalinkina, E.V., Kalinkin, A.M., Forsling, W., and Makarov, V.N., *Int. J. Miner. Process.*, 2001, vol. 61, pp. 273–288.
23. Karickhoff, S.W. and Bailey, G.W., *Clay Clay Miner.*, 1976, vol. 24, pp. 170–176.
24. Poli, L., Batista, T., Schmitt, C.C., Gessner, F., and Neumann, M.G., *J. Colloid Interf. Sci.*, 2008, vol. 325, pp. 386–390.